# SEISMIC BEHAVIOR OF CONCRETE BEAMS WITH DIFFERENT TYPES OF HOOPS IN THE PLASTIC HINGE REGION

## Beams, seismic, hoops, detailing

Yu-Chen Ou[1], Hermawan Sutejo[2], and Jyun-Lin Huang[3]

Hoops should be provided in the plastic hinge region of beams of the special moment frame. However, the conventional hoop configuration in accordance with the code causes difficulties in hoop installation and arrangements during construction. In this research, a total of five beam specimens with different types of hoops were tested under cyclic loading. One specimen was applied with conventional hoops (specimen S1). Three specimens were designed with innovative hoops that improve constructability. The innovative hoop of specimens S2, SL1, and SL2 was characterized by a continuous bar forming the outer stirrup and inner hoop, by two U stirrups lap spliced to form the inner hoop by two three-dimensional stirrups lap spliced to form the inner hoops, respectively. One specimen was equipped with two overlapping perimeter hoops (specimen S3), which are common in Taiwan but do not satisfy the code requirements. The results showed that the three main bars enclosed by the inner hoops of specimens S2, SL1, and SL2 were effectively restrained. As the drift ratio of the beam reached 6%, the main bars and the inner hoops were fractured in the buckling region. Relative to specimen S1, the ultimate drift ratio ($\Delta_u$) of specimens S2, SL1, and SL2 were higher by 1%, 8%, and 13%, respectively. At the drift ratio of 4%, the equivalent damping ratios ($\xi_{eq}$) of specimens S2, SL1, and SL2 were higher by 10%, 12%, and 14%, respectively, compared to specimen S1. Although the concrete in the plastic hinge region had cracked and showed some spalling, the lap splices of the inner hoops of specimens SL1 and SL2 were sufficiently confined by the concrete core, which enabled the lap-spliced hoops to reach the yield strain. Thus, a ductile flexural failure was observed. On the contrary, as the drift ratio of the beam reached 5%, specimen S3 was severely damaged, most of the main bars were severely buckled, and the concrete core was severely cracked. Relative to specimen S1, the $\Delta_u$ of specimen S3 was 15% lower. In terms of equivalent damping ratio, when the beam reached the drift ratio of 4%, the $\xi_{eq}$ of specimen S3 is lower by 6% relative to specimen S1. The strength of the beam deteriorated rapidly as the main bars capped by crossties were subjected to high compression. Specimen S3 failed to satisfy the seismic performance evaluation of ACI 374.1-05.

***Keywords:*** *reinforced concrete beams, seismic, reinforcement buckling, hoops, plastic hinge region, drift capacity, energy dissipation, special moment frame*

[1] Distinguished Professor, Department of Civil Engineering, National Taiwan University, Taiwan
[2] Ph.D. Candidate, Department of Civil Engineering, National Taiwan University, Taiwan
[3] M.S., Department of Civil Engineering, National Taiwan University, Taiwan

## EXPERIMENTAL PLAN

### Specimen Design and Fabrication

Five large-sized specimens of beams of ACI 318-19[1] special moment frames were fabricated. The dimensions of all specimen cross-sections were 700x900 mm. The specimen dimensions, heights, longitudinal reinforcement sizes, and configurations were identical for all five beam specimens. The experimental variable was the type of hoops, which was the only difference among the five beam specimens. The design compressive strength of concrete ($f_{cd}{}'$) was 35 MPa, and the design yield strength of reinforcement ($f_{yd}$) was 420 MPa. **Figure 1** shows the specimen design of S1. The longitudinal reinforcement comprised seven D32 bars near the north and south side of the beam section. The tensile longitudinal reinforcement ratio was 0.98%. The perimeter and inner hoops used D13 bars for all specimens except the inner hoop of specimen SL1, which used D12 deformed-wire reinforcement with the design yield strength ($f_{yd}$) of 500 MPa. The maximum hoop spacing is 150 mm, conforming to the maximum spacing requirement for the potential plastic hinge region of beams of ACI 318-19 [1] special moment frames.

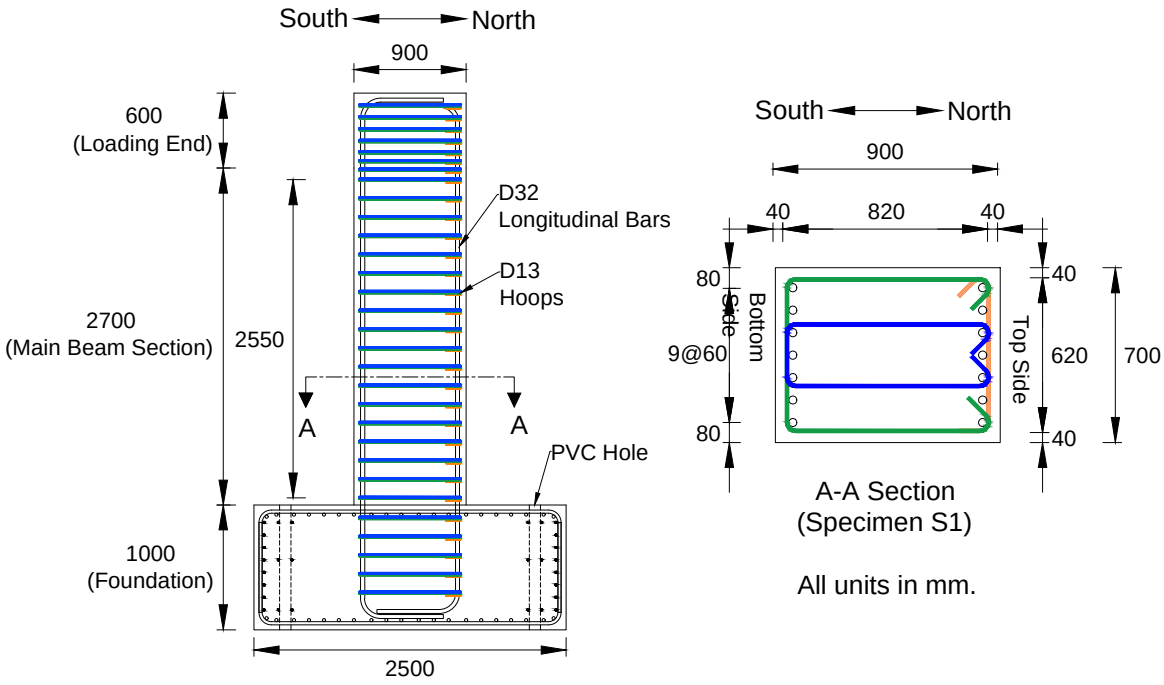


**Figure 1.** Specimen design

All specimens were designed to exhibit flexural failure. The ratio between shear force due to the probable flexural strength of the beam ($V_{pr}$) and the design shear strength ($\phi V_n$) is 87%. This critical design aimed to observe whether the hoops developed full shear strength.

In terms of hoop design, specimen S1 was applied with conventional hoops, each set consisting of an outer and inner stirrup closed by a crosstie (**Fig. 2a**). Specimen S2, specimen SL1, and specimen SL2 used innovative hoops. Each set of the hoop of specimen S2 was formed by a stirrup with a continuous bar forming the outer stirrup and inner hoop and by a crosstie to close the outer stirrup (**Fig. 2b**). Specimens SL1 and SL2 used the same outer stirrup closed by a crosstie as the previous two specimens. However, specimens SL1 and SL2 used lap splice to

form the inner hoop. In specimen SL1, two U stirrups were lap spliced to form the inner hoop, as shown in **Fig. 2(c)**, while in specimen SL2, two three-dimensional stirrups were lap-spliced to create the inner hoops, as shown in **Fig. 2(d)**. The lap-splice length of SL1 and specimen SL2 was set to be $1.3l_d$. It was based on the ACI 318-19 class B tension lap-splice length.

On the other hand, specimen S3 was designed based on common practice in Taiwan but failed to satisfy the requirement of section 25.7.2.3(a) of ACI 318-19, which specifies that the corner of a tie should laterally support every corner and alternate longitudinal bar with an included angle, not more than 135 degrees. Moreover, the clear distance between unsupported bars should not be larger than 150 mm on each side along the tie.

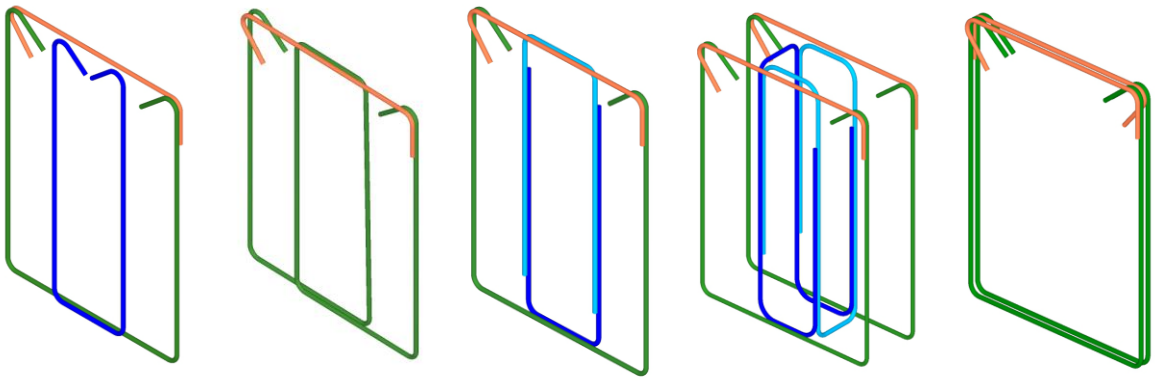

(a) S1 (b) S2 (c) SL1 (d) SL2 (e) S3

**Figure 2.** Hoop configuration

**Test Setup**

**Figure 3** and **Figure 4** show the loading history and the test setup, respectively. Per ACI 374.1[2], the actuator applied three cycles for each drift ratio in the north-south direction. The displacement load increased incrementally. The drift ratio in the south direction was defined as a positive drift ratio and in the north direction as a negative drift ratio. The drift ratio was defined as the lateral drift divided by the vertical distance between the upper face of the foundation to the actuator. The test was terminated when the specimen was severely damaged or the strength dropped below 50%.

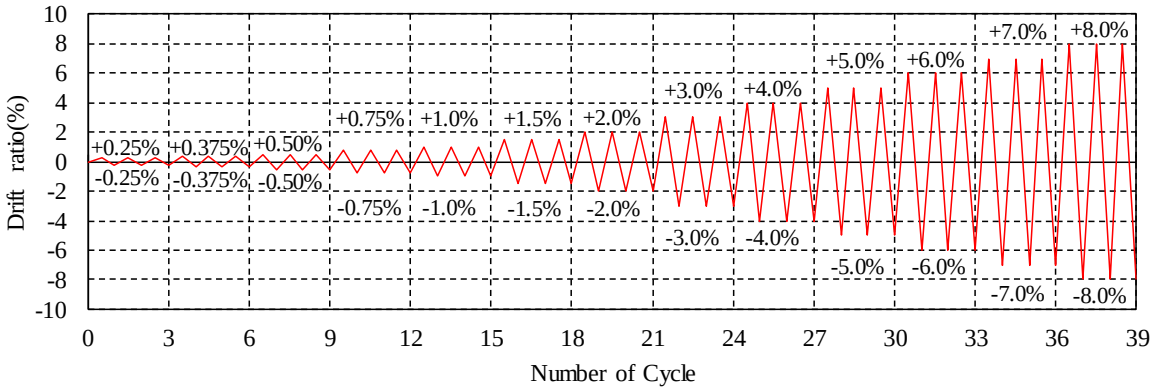


**Figure 3.** Loading history

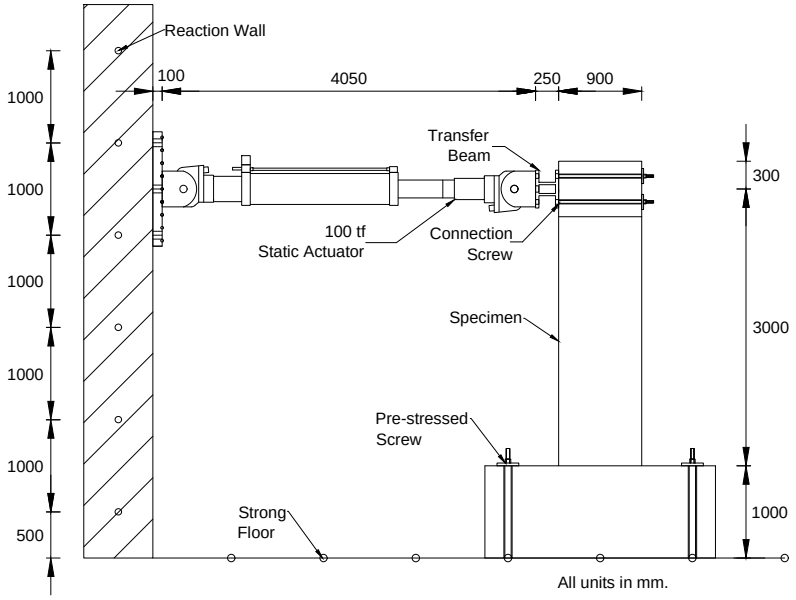


**Figure 4.** Test setup

## EXPERIMENTAL RESULTS AND ANALYSIS

### Hysteresis Results and Envelope

The strength of specimen S3 decreased significantly to 82% when the drift ratio reached 4%, as shown in **Figure 5**. The other specimens still showed increasing strength. Slight longitudinal bar buckling and concrete cover spalling occurred at the top side of specimen S3. As the drift ratio reached 5%, the strengths of the specimens in terms of a percentage to the peak strength sorted in ascending order were specimens S3(61%), S1(85%), SL1(90%), S2(91%), and SL2(94%).

Concerning longitudinal reinforcement failure, seven of specimen S3 top longitudinal bars and five of specimen S1 longitudinal bars had severely buckled. Specimens S2, SL1, and SL2 performed the best, with buckling occurring at only four longitudinal bars. Concerning concrete failure, at a drift ratio of 5%, specimens S1 and S3 top concrete cover spalling were similar. The concrete cover spalling area length was 110 cm for specimens S1 and S3 and 95 cm (14% lower) for specimens with innovative inner hoops (S2, SL1, and SL2). Moreover, the concrete core of specimen S3 was critically cracked on the north and south faces.

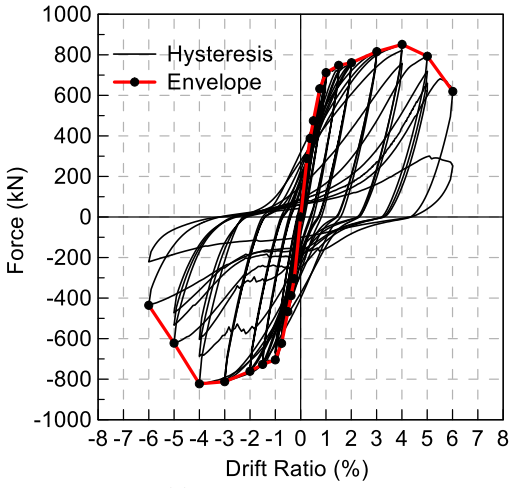


(a) Specimen S1

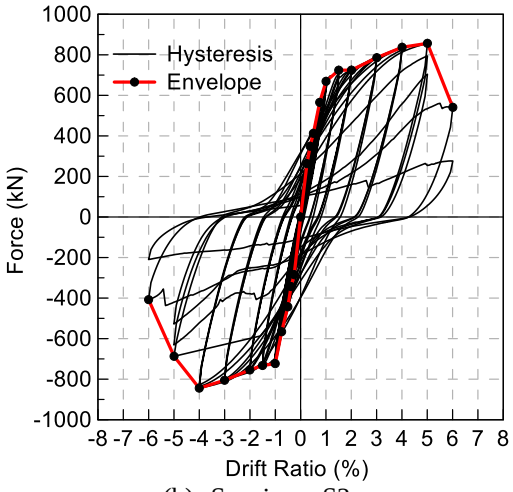


(b) Specimen S2

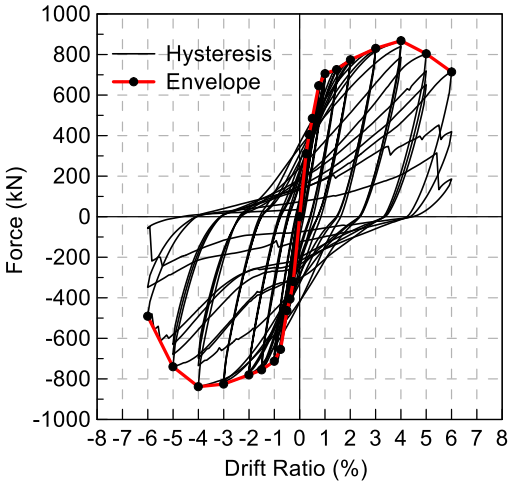


(c) Sepcimen SL1

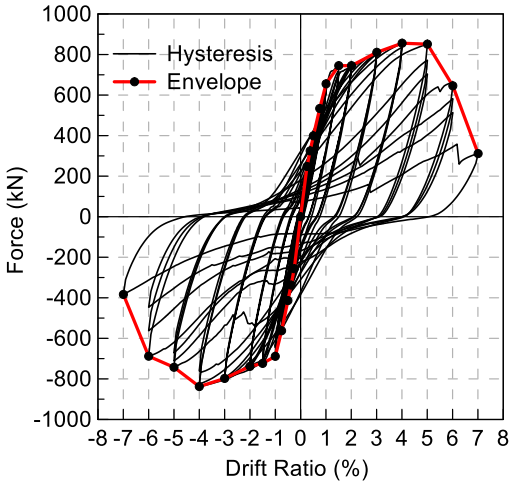


(d) Specimen SL2

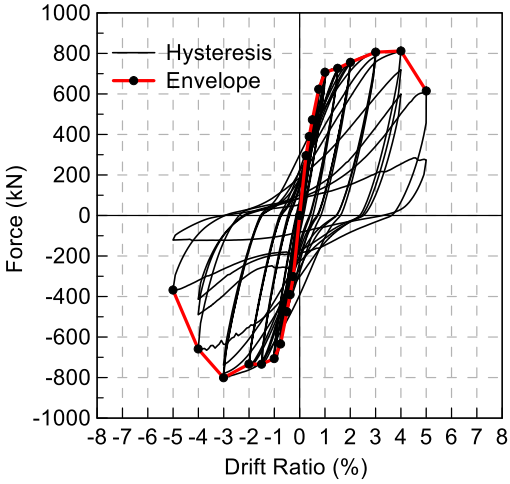


(e) Specimen S3

**Figure 5.** Hysteresis and envelope curves of all specimens

(a) Specimen S1

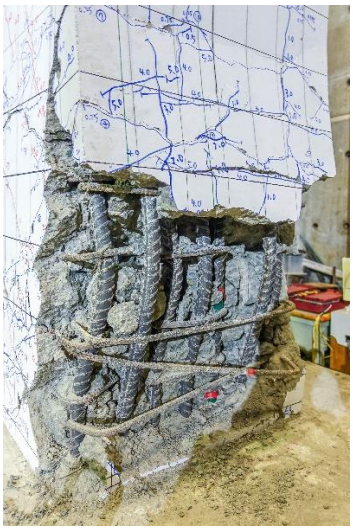

(b) Specimen S2

(c) Specimen SL1

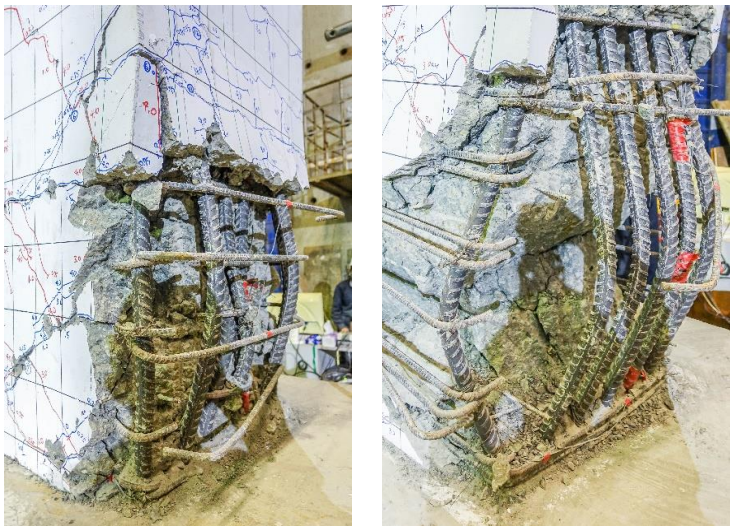

(d) Specimen SL2 (e) Specimen S3

**Figure 6.** Buckling of top longitudinal bars of all specimens at a drift ratio of 5%

**Figure 6** shows the specimens conditions at a 5% drift ratio. The inner hoops of specimen S1 retained two longitudinal bars effectively, while the inner hoops of specimens S2, SL1, and SL2 restrained three longitudinal bars. As for specimen S3, all longitudinal bars had been buckled since the double overlapping perimeter hoops could no longer restrain all longitudinal bars. After the 5% drift ratio, the strength of specimen S3 deteriorated to lower than 50%. Hence the test was terminated. After the test, the longitudinal bars and the inner hoops of specimens S2, SL1, and SL2 had fractured. The cracks developed in specimens SL1 and SL2 with innovative hoops were the less severe among all specimens.

**Bilinear Model and Force Analysis**

The bilinear analysis was based on FEMA 356[3] Chapter 3. The envelope curve was idealized by the bilinear model for ductility analysis, as illustrated in **Figure 7.** The strength ratio ($M_{test}/M_n$) was the ratio of the maximum moment obtained from the test ($M_{test}$) to the nominal moment capacity ($M_n$). The nominal moment capacity was measured based on the actual strength of the materials.

**Table 1** shows the ductility assessment results and the bilinear model of each specimen. Relative to the control specimen (S1), the $\Delta_y$ of specimens S2, SL1, and SL2 were 16%, 2%, and 24% higher, respectively. The $\Delta_u$ of specimens S2, SL1 and SL2 were 1%, 8%, and 13% higher than specimen S1. As for $\Delta_p$, specimens with lap-spliced inner hoops (SL1 and SL2) were higher by 9% and 11% relative to specimen S1, while specimen S2 was 2% lower than specimen S1. Contrastingly, the $\Delta_y$, $\Delta_u$ and $\Delta_p$ of specimen S3 was lower by 6%, 15%, and 17%, respectively, compared to specimen S1.

Strength ratios ($M_{test}/M_n$) of all specimens were larger than 1. The results indicated that specimens S2, SL1, and SL2 possessed higher ductility because the innovative inner hoops effectively restrained the three longitudinal bars at the center of the cross-section. On the contrary, specimen S3 could not develop ductility because the buckling of the main reinforcement and the concrete cracks occurred early.

**Table 1.** Ductility assessment comparison

| Specimen | S1 | S2 | SL1 | SL2 | S3 |
|---|---|---|---|---|---|
| $\Delta_y$ (%) | 0.82 | 0.95 | 0.84 | 1.02 | 0.77 |
| $\Delta_u$ (%) | 5.24 | 5.30 | 5.66 | 5.94 | 4.45 |
| $\mu$ | 6.38 | 5.58 | 6.81 | 5.84 | 5.76 |
| $\Delta_p$ (%) | 4.42 | 4.35 | 4.83 | 4.92 | 3.68 |
| $V_y$ (kN) | 774 | 776 | 793 | 780 | 746 |
| $V_{max}$ (kN) | 837 | 850 | 853 | 847 | 806 |
| $M_{test}/M_n$ | 1.21 | 1.23 | 1.23 | 1.23 | 1.17 |

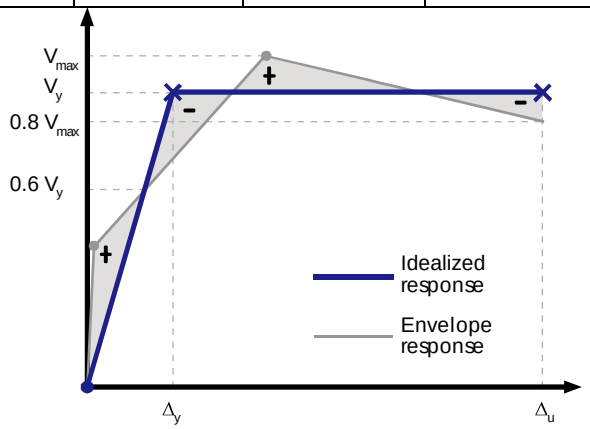


**Figure 7.** Bilinear model illustration

**Energy Dissipation**

The equivalent damping ratio ($\xi_{eq}$) was calculated by Eq. (1), as illustrated in **Figure 8** (a). The calculation of $\xi_{eq}$ is based on FEMA 356 [3] Chapter 9. The area enclosed by the first cycle of the hysteresis curve is the dissipated energy denoted by $E_D$. The area covered by the triangle in **Figure 8** (a) is the effective strain energy, $E_S$.

$$\xi_{eq} = \frac{1}{4\pi}\left(\frac{E_D}{E_S}\right) \quad (1)$$

**Figure 8** (b) shows the equivalent damping ratio of each specimen. After the 4% aspect ratio, the $\xi_{eq}$ started to decrease. In comparison with specimen S1 at a 4% drift ratio, the $\xi_{eq}$ of specimens S2, SL1, and SL2 were higher by 10%, 12%, and 14%, respectively. On the other hand, the $\xi_{eq}$ of specimen S3 was lower by 6% than specimen S1.

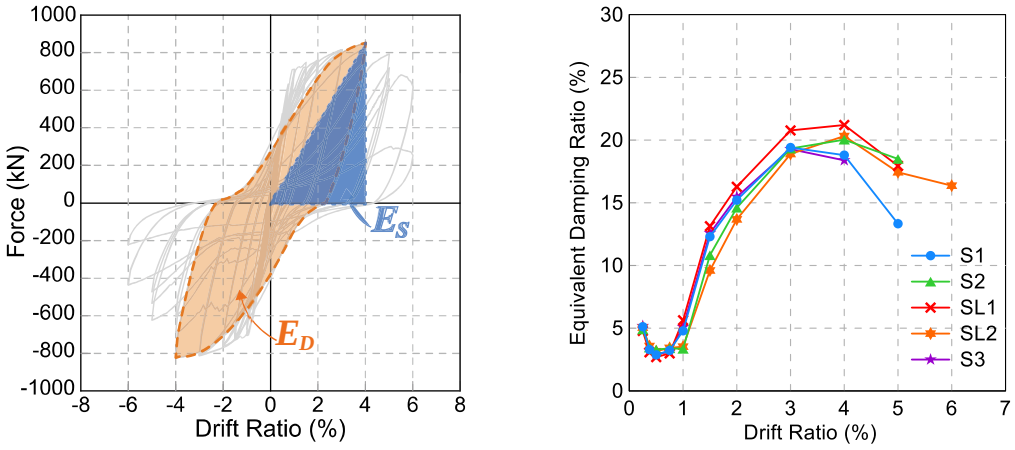


(a) Illustration of equivalent damping

(b) The equivalent damping ratio of each specimen

**Figure 8.** Equivalent damping ratio

## CONCLUSIONS

This research involved five specimens with different types of hoops under a cyclic loading test. One specimen was applied with conventional hoops (specimen S1). Three specimens were designed with innovative hoops that improve constructability. The innovative hoop of specimens S2, SL1, and SL2 was characterized by a continuous bar forming the outer stirrup and inner hoop, by two U stirrups lap spliced to form the inner hoop by two three-dimensional stirrups lap spliced to form the inner hoops, respectively. One specimen was equipped with two overlapping perimeter hoops (specimen S3), which are common in Taiwan but do not satisfy the code requirements. From the test results, the following conclusions can be drawn:

1. Experimental results and envelope

   At a drift ratio of 5%, specimen S1 with conventional inner hoops restrained 2 longitudinal bars at the center of the cross-section. While the innovative inner hoops of specimens S2, SL1, and SL2 restrained 3 longitudinal bars at the center of the cross-section, showing that the reinforcing bars fully exerted energy dissipation. On the other hand, all longitudinal bars of specimen S3 had buckled. At a drift ratio of 6%, longitudinal bars and inner hoops fracture occurred at the buckling region. For specimens SL1 and SL2 with lap-spliced inner hoops, three longitudinal bars at the center of the cross-section were effectively restrained, indicating that the lap-splices length was sufficient to ensure flexural failure took place rather than shear failure. Specimen S3, with overlapping double perimeter hoops, failed to restrain the longitudinal bars, and the concrete confinement was poor, resulting in the severe buckling of the longitudinal bars and serious concrete cracks. As specimen S3 suffered severe damage, the contribution of the cross-sectional area effective in resisting compression reduced significantly, resulting in the specimen strength failing earlier.

2. Bilinear model and force analysis

   Relative to the control specimen (S1), the $\Delta_y$ of specimens S2, SL1, and SL2 were higher by 16%, 2%, and 24%, respectively, $\Delta_u$ were higher by 1%, 8%, and 13%, respectively. As for $\Delta_p$, compared to specimen S1, specimens with lap-spliced inner hoops (SL1 and SL2) were 9% and 11% higher, respectively. On the other hand, the $\Delta_p$ of specimen S2 were lower by 2% in comparison with specimen S1. On the contrary, the $\Delta_y$, $\Delta_u$, and $\Delta_p$ of specimen S3 were lower by 6%, 15%, and 17%, respectively, compared to specimen S1. As the longitudinal bars buckled and the concrete cracked earlier, specimen S3 could not develop ductility.

3. Energy dissipation

   At a 4% drift ratio, the energy dissipation of every specimen started to drop because the concrete spalling had occurred and the main reinforcement initiated buckling. In comparison with specimen S1 at a 4% drift ratio, the $\xi_{eq}$ of specimens S2, SL1, and SL2 were higher by 10%, 12%, and 14%, respectively. Contradictorily, the $\xi_{eq}$ of specimen S3 was 6% lower than specimen S1.

## ACKNOWLEDGEMENT

This research was funded by Chien Kuo Construction Co., Ltd., and the National Center for Research on Earthquake Engineering (NCREE) provided test equipment and sites.

**NOTATIONS LIST**

| | |
|---|---|
| $E_D$ | Total energy dissipated in the isolation system per displacement cycle |
| $E_S$ | Effective strain energy |
| $f'_{cd}$ | Design compressive strength of concrete |
| $f_{yd}$ | Design yield strength of reinforcement |
| $M_n$ | Beam nominal moment capacity |
| $M_{test}$ | Beam maximum moment from testing |
| $V_{max}$ | Maximum test lateral force |
| $V_n$ | Beam nominal shear strength |
| $V_{pr}$ | Beam probable flexural strength |
| $V_y$ | Beam effective yield strength |
| $\Delta_p$ | Plastic drift ratio |
| $\Delta_u$ | Drift ratio at the ultimate point |
| $\Delta_y$ | Drift ratio at the yield point |
| $\mu$ | Ductility |
| $\xi_{eq}$ | Equivalent damping ratio |

**REFERENCES**


1. Committee, A.C.I., *Building code requirements for structural concrete and commentary (ACI 318-19)*. American Concrete Institute: Farmington Hills, MI, USA. 2019. 623.
2. Committee, A., *Acceptance criteria for moment frames based on structural testing and commentary*. 2005. **374**: p. 1-05.
3. Engineers, R., *FEMA 356: prestandard and commentary for the seismic rehabilitation of buildings, Report No.* FEMA, 2000.